

Comparator Factors for Single Standardization Techniques in Elemental Analysis of Archaeological Matrices

Njinga R.L.¹, Jonah S.A.², Oladipo M.O.A.², Ewa I.O.B.², Alfa B.¹

¹Physics Department, Ibrahim Badamasi Babangida University, Lapai, Niger State, Nigeria

²Center for Energy Research and Training, Ahmadu Bello University, Zaria, Nigeria

ABSTRACT

The evaluations of comparator factors (F_c) in irradiation position of a nuclear research reactor provide accurate bases for elemental concentration in any form of matrices. These values have been experimented to be very close to theoretical values. This implies that the k_0 -INAA and k_0 -ENAA technique employed in this work shows no irregularities in the obtained efficiency, data-entry, decay time used, and the dead time of $< 6\%$. The experimental value in inner irradiation position (B-2) is $7.120E+05$ while theoretical value is $7.330E+05$ with a percentage deviation of 2.86 (from theoretical value). In large outer irradiation position (A-3) we obtained the experimental value of $1.170E+06$ and the theoretical value of $1.210E+06$ with a percentage deviation of 3.310 (from theoretical value). The experimental values were obtained using Au (0.1%) - Al monitor foil and a neutron flux setting of $5.00E+11 \text{ cm}^{-2}\cdot\text{s}^{-1}$. A further analysis of ten archaeological samples using k_0 -ENAA technique revealed that the concentration of U/Np, Th/Pa and K (dose rate) increases inwardly from the earth surface.

Keywords: Flux distribution, Cadmium lined, Specific Activity Ratio, NIRR-1, dose rate, research reactor.

1. INTRODUCTION

The miniature nuclear research reactors are the most efficient neutron sources for high sensitivity activation analysis induced by thermal, epithermal and fast neutrons (Jonah et al., 2005).

The Nigeria Research reactor-1 (NIRR-1) at the Centre for Energy Research and Training (CERT), ABU Zaria-Nigeria is extensively used for neutron activation analysis (NAA). The reactor has a nominal core power of 31kW and uses de-ionized light water as the coolant/moderator. The neutron flux at inner irradiation sites is approximately $1 \times 10^{12} \text{ cm}^{-2}\cdot\text{s}^{-1}$ with stability range of $\pm 1\%$, horizontal and vertical variation of $< 3\%$. At the moment, the control rod is one stainless steel clad, cadmium absorber. The temperature in the irradiation sites are; inner site $< 54^\circ\text{C}$; outer sites $< 40^\circ\text{C}$ (at pool temperature of 20°C). The core reactivity temperature coefficient is $-0.1 \text{ mk}^\circ\text{C}$ and the core temperature ranged from 15°C to 40°C (Balogun, 2003). The reflector is of metallic beryllium and it comprises of 10 sites (5 inner and 5 outer) 6 sites connected (4 inner and 2 outer). This reactor is essentially employed for researches such core modification, characterizations to expand scope of applications such as large number of elements, less cost, short-turnaround time, less use of standards, modifications of existing techniques and so on as this work seek to address.

The comparator factor (F_c) is an essential parameter when calculating the concentration of sample using k_0 -standardization method in the neutron activation analysis (NAA). This factor (F_c) is proportional to thermal, epithermal flux and is independent of monitor element, detection efficiency. The factor (F_c) allows averaging and gives information on flux gradients (several monitors in a irradiation vial), and flux stability (monitor history). This is very important because it detects any gross irregularities in efficiency, data-entry, decay times (De Corte et al., 2004). Thus, as aimed in this work, the comparator factor was analyzed theoretically and experimentally through the $^{197}\text{Au} (n, \gamma) ^{198}\text{Au}$ and $^{27}\text{Al} (n, p) ^{27}\text{Mg}$ reactions respectively in both inner irradiation channel B-2 without Cd-liner and outer channel A-3 with Cd-liner. This was achieved by measuring the activity of irradiated thin 0.1% Au-Al foil monitor.

2. MATERIALS AND METHODS

The theoretical basics in evaluation of elemental concentration in any form of matrices qualitatively or quantitatively using k_0 -INAA or k_0 -ENAA techniques depends on Equation 1 and 2. For analysis in a non Cd-lined channel, B-2, Equation 1 is used given as (De Corte et al., 1996);

$$conc(a) = \frac{\left(\frac{N_p}{t_m SDCm}\right)_a}{\left(\frac{N_p}{t_m SDCm}\right)_m} \times \frac{1}{k_{o,m}(a)} \times \frac{f + Q_{o,m}(\alpha)}{f + Q_{o,a}(\alpha)} \times \frac{\varepsilon_{p,m}}{\varepsilon_{p,a}} \times 10^6 \quad (1)$$

However, based on the performance of k_0 -based Epithermal Cadmium Neutron Activation Analysis (EpiCd-NAA) in the Cd-lined channel (A-3), Equation 2 is used given as (De Corte et al., 1996);

$$conc(a) = \frac{\left(\frac{N_p}{t_m SDCm}\right)_{Cd}}{\left(\frac{N_p}{t_m SDCm}\right)_m} \times \frac{1}{k_{o,m}(a)} \times \frac{F_{Cd,m} Q_{o,m}(\alpha)}{F_{Cd,a} Q_{o,a}(\alpha)} \times \frac{\varepsilon_{p,m}}{\varepsilon_{p,a}} \times 10^6 \quad (2)$$

where the subscripts “a” and “m” stands respectively for the analytic and the co-irradiated monitor $^{197}\text{Au}(n, \gamma)^{198}\text{Au}$ with properties $Q_0 = 15.7$; $T_{1/2} = 2.695$ d; $E_\gamma = 411.8$ keV

N_p = net peak count corrected for pulse losses,

t_m = measuring time,

$k_{o,m}(a)$ = k_0 factors of “a” and “m”,

F_{Cd} = cadmium transmission factor for epithermal neutrons.

From Eq. 1 and 2, we obtained the comparator factors (F_c) respectively as;

$$F_{c,Au} | (without Cd - lined) = \frac{\left(\frac{N_p / t_{measuring}}{SDCW}\right)_m}{k_{0,Au}(m)} \cdot \frac{1}{G_{th,m} \cdot f + G_{th,m} \cdot Q_{0,m}(\alpha)} \cdot \frac{1}{\varepsilon_{p,m}} \times 10^{-6} \quad (3)$$

$$F_{c,Au} | (with Cd - lined) = \frac{\left(\frac{N_p / t_{measuring}}{SDCW}\right)_m}{k_{0,Au}(m)} \cdot \frac{1}{F_{Cd,m} \cdot G_{e,m} \cdot Q_{0,m}(\alpha)} \cdot \frac{1}{\varepsilon_{p,(m)}} \times 10^{-6} \quad (4)$$

In measurement of thermal neutron spectrum flux (Φ_{th}) and epithermal neutron flux (Φ_{epi}), we used the following Equations (5 and 6) respectively (Njinga et al., 2012);

$$\Phi_{th} = \frac{N_p \lambda M}{(1 - e^{-\lambda t_{irr}}) \times (e^{-\lambda t_c}) \times (1 - e^{-\lambda t_m}) \times \sigma_{th} \left(1 + \frac{Q_0(\alpha)}{f}\right) \times \theta \times \gamma \times N_A \times w \times \varepsilon_p \times c} \quad (5)$$

$$\Phi_{epi} = \frac{N_p \lambda M}{(1 - e^{-\lambda t_{irr}}) \times (e^{-\lambda t_c}) \times (1 - e^{-\lambda t_m}) \times I_0(\alpha) \times \theta \times \gamma \times N_A \times w \times \varepsilon_p \times c} \quad (6)$$

Making used of equation Eq. 3 and 5, we obtained the comparator factor in the inner irradiation channel B-2 without Cd-line given as;

$$F_{c,Au} = \frac{N_A \cdot \theta_{Au} \cdot \sigma_{0,Au} \cdot \gamma_{Au}}{M_{Au}} \cdot \frac{\Phi_{th}}{f} \cdot 10^{-6} \quad (7)$$

Making used of equation Eq. 4 and 6, we obtained the comparator factor in the installed Cd-line channel A-3 given as;

$$F_{c,Au} = \frac{N_A \cdot \theta_{Au} \cdot \sigma_{0,Au} \cdot \gamma_{Au}}{M_{Au}} \cdot \Phi_{epi} \cdot 10^{-6} \quad (8)$$

where θ = isotopic abundance, λ = decay constant = $\ln 2 / T_{1/2}$, c = concentration of foil monitor, ε_p = peak efficiency, γ = gamma abundance, w = weight of foil monitor, t_{irr} = irradiation time, t_c = cooling time after irradiation, t_m = measuring time, M = atomic weight, N_A = Avogadro's number, N_p = net peak area, σ_{th} = thermal cross section,

3. EXPERIMENTS

Two monitors made of 0.1% Au-Al foil alloy; 0.1 mm thick, IRRM-530; weight from 0.0129 to 0.0134 g were irradiated in turn in Cd-lined outer irradiation channel and

inner irradiation channel of NIRR-1. The irradiation of the Au-0.1% Al foils were done in A-3 and B-2 only. In B-2 (without Cd-lined), the irradiation time was 1800 seconds; while in A-3 (with Cd-lined) the irradiation was 7200 seconds (Table 1). Measurements of Au-0.1% Al foil irradiated in B-2 and A-3 were performed for the first count at 17cm from the GEM-30195 detector’s end-cap for 600 seconds each; while for the second count, measurements were carried out at 2cm distance for 1800 seconds each (Table 2). The results of the specific activity in terms of nuclear reaction; $^{27}\text{Al}(n, p)^{27}\text{Mg}$ (1014 keV, 843 keV; $T_{1/2}=9.46\text{mins}$), $^{27}\text{Al}(n, \alpha)^{24}\text{Na}$ (1368.6 keV, $T_{1/2}=14.96\text{hrs}$) $^{197}\text{Au}(n, \gamma)^{198}\text{Au}$ (411.80 keV; $T_{1/2}=2.7\text{days}$) are shown in Table 1 and 2 below (the nuclear data such as the half-lives, peak energy were obtained from Erdtmann and Soyka, 1978; Glasscock, 1988).

The outer irradiation channel A-3 with Cd-lined was further employed to activate twelve including two standard reference sediments archeological samples for dose rate measurements. The samples were grouped into sets of six sample-matrices comprising standard reference materials. The summary of the irradiations and counting schedules are shown in Table 5, 6, 7, 8, 9 and 10.

4. RESULTS AND DISCUSSIONS

After appropriate cooling time, the specific activity based on nuclear data; 1014 keV, 843 keV; $T_{1/2} = 9.46\text{mins}$ for $^{27}\text{Al}(n, p)^{27}\text{Mg}$ reaction; 1014 keV, 843 keV; $T_{1/2}=9.46\text{mins}$ for $^{27}\text{Al}(n, \alpha)^{24}\text{Na}$ nuclear reaction; 411.80 keV; $T_{1/2}=2.7\text{days}$ for $^{197}\text{Au}(n, \gamma)^{198}\text{Au}$ nuclear reaction are shown in Table 1 and 2 (Glasscock, 1988).

Table 1: Specific Activity measurement in two irradiation channels using $^{27}\text{Al}(n,p)^{27}\text{Mg}$ and $^{27}\text{Al}(n,\alpha)^{24}\text{Na}$

Channels	Irradiation time, (s)	Cooling time, (s)	T_m (s)	Sample ID	Weight (g)	Peak Energy (KeV)	Specific activity (Bq/g)
A-3 (Cd-lined) ^a	7200.00	480.00	600.00	069M188	0.013	1014.00	253.55
A-3 (Cd-lined) ^b	7200.00	75120.00	1800.00	069M188	0.013	1368.60	1945.25
B-2 Inner ^a	1800.00	1140.00	600.00	069M186	0.012	1014.00	2163.72
B-2 Inner ^b	1800.00	76740.00	1800.00	069M186	0.012	1368.60	13801.99
B-2 Inner ^a	1800.00	1140.00	1800.00	069M186	0.012	843.00	6384.74

Table 2: Specific Activity measurement in two Irradiation channels using $^{197}\text{Au}(n,\gamma)^{198}\text{Au}$

Channels	Irradiation time, (s)	Cooling time, (s)	T_m (s)	Sample ID	Weight (g)	Peak Energy (KeV)	Specific activity (Bq/g)
A-3 (Cd-lined) ^a	7200.00	480.00	600.00	069M188	0.013	411.80	31840.75
A-3 (Cd-lined) ^b	7200.00	75120.00	1800.00	069M188	0.013	411.80	460734.77
B-2 Inner ^a	1800.00	1140.00	600.00	069M186	0.012	411.80	421037.51
B-2 Inner ^b	1800.00	76740.00	1800.00	069M186	0.012	411.80	5714584.96

^a = represent first measurements at 17 cm, ^b = represent second measurements at 2 cm, T_m = Measurement time

The experimental values of f , Φ_{th} , and Φ_{epi} for the two irradiation channels A-3, B-2, at a neutron thermal flux rate of $5.0E+11$ n/cm²s on the control console has been published by Njinga et al., (2012). All the nuclear data used in this computation were obtained from the Table for neutron activation analysis (Glasscock, 1988). These values were used in reference to Eq. 7 and 8 to obtain the theoretical values of the comparator factors in the two channels (B-2 and A-3) results shown in Table 4. The $Q_{0,^{198}\text{Au}}$ values employed were α -corrected based on the relationship;

$$Q_{0,^{198}\text{Au}}(\alpha) = \frac{15.71 - 0.429}{(5.65)^\alpha} + \frac{0.429}{(2\alpha + 1)(0.55)^\alpha}$$

These values obtained in B-2 and A-3 are shown in Table 3 below.

The experimental evaluations of comparator factor F_c were measured in accordance to Equation 3 and 4 and making used of Table 1, 2, & 3. The experimental results of F_c are shown in Table 4.

Table 3: $Q_0(\alpha)$ values obtained for Au

Irradiation Positions	B-2	A-3
Pro-Isotope	^{198}Au	^{198}Au

Reaction	$^{197}\text{Au}(n, \gamma)$	$^{197}\text{Au}(n, \gamma)$	Cd-Cut off Energy	0.550	0.550
Resonance Energy (eV)	5.700	5.700	Q_0	15.700	15.700
Epitherma Factor	Shape -0.052	-1.274	$Q_0(\alpha)$	17.210	139.640
Thermal Cross Section	98.700	98.700			

Table 4: Comparator factors of B-2 and A-3 Irradiation Channels

Irradiation Channels	Irradiation Time (sec)	Cooling Time (sec)	Comparator Factor (Fc)		Deviation from Theoretical values
			Experimental	Theoretical	
B-2	1800.000	1140.000	7.120E+05	7.330E+05	2.860E-02
A-3	7200.000	480.000	1.170E+06	1.210E+06	3.310E-02

Table 5: Irradiation schedules for first sets of Six Archaeological Samples in A-3

Sample type	Weight (g)	T_{irr} (hrs)	T_{in} (am)	T_{end} (pm)
Coal fly ash (1633b)	0.583	6.000	10:41	16:41
800Tat. 5 th	0.645	6.000	10:41	16:41
600Tat. 6 th	0.613	6.000	10:41	16:41
200Tat. 3 rd	0.606	6.000	10:41	16:41
4 th Tat. 1HYS	0.614	6.000	10:41	16:41
100Tat. 2 nd	0.623	6.000	10:41	16:41

Table 6: Irradiation schedules for the 2nd sets of Six Archaeological Samples in A-3

Sample type	Weight (g)	T_{irr} (hrs)	T_{in} (am)	T_{end} (pm)
3 rd Tat. 2YS	0.538	6.000	10:09	16:09
1 st Tat. MRB	0.536	6.000	10:09	16:09
2 nd Tat. AHM3	0.626	6.000	10:09	16:09
45 Tat. 1 st	0.646	6.000	10:09	16:09
400Tat. 4 th	0.506	6.000	10:09	16:09
IAEA lake sediment	0.547	6.000	10:09	16:09

T_{irr} = irradiation time, T_{in} = Initial irradiation time, T_{end} = Final irradiation time

The induced activities in the samples were measured using a vertical dip-stick detector ORTEC-GEM-30195 HPGe coaxial, with resolution (FWHM) at 1.33 MeV, ^{60}Co to be 1.85 keV and at 122 keV, ^{57}Co to be 0.85 keV, peak-to-Compton ratio, ^{60}Co to be 60:1 and relative efficiency of 30 % at 1332.5 keV of ^{60}Co at a geometry of 25cm.

The measurements of the two sets of activated samples were performed in two geometries each, after a waiting

period of 3 to 5 days. The first measurements of both the first and second groups were performed at 2 cm for medium and long lived nuclides after three days for 1800 seconds (Table 7 and 8). The second measurements of both groups were measured at 2 cm after five days for long half lived nuclides for 3600 seconds (Table 9 and 10). The dead time of each measurement did not exceed 6% and the peak statistic was above 0.5% (Jonah et al., 2005).

Table 7: Counting schedules for first sets of Six Archaeological Samples after 3 days

Sample type	T_{begin}	T_{live} (sec)	T_{real} (sec)	Geom. (cm)
Coal fly ash (1633b)	09:26AM	1800.00	1851.420	2.000

800Tat. 5 th	10:01AM	1800.00	1879.420	2.000
600Tat. 6 th	10:34AM	1800.00	1838.640	2.000
200Tat. 3 rd	11:07AM	1800.00	1834.660	2.000
4 th Tat. 1HYS	11:39AM	1800.00	1855.380	2.000
100Tat. 2 nd	12:12PM	1800.00	1830.840	2.000

Table 8: Counting schedules for the 2nd sets of Six Archaeological Samples after 3 days

Sample type	T _{begin}	T _{live} (s)	T _{real} (s)	Geom. (cm)
3 rd Tat. 2YS	09:48AM	1800.00	1818.64	2.000
1 st Tat. MRB	10:27AM	1800.00	1814.56	2.000
2 nd Tat. AHM3	11:07AM	1800.00	1858.66	2.000
45 Tat. 1 st	11:48AM	1800.00	1832.00	2.000
400Tat. 4 th	12:32PM	1800.00	1851.58	2.000
IAEA lake sediment	14:19PM	1800.00	1824.40	2.000

Table 9: Counting schedules for 1st sets of Six Archaeological Samples after 5 days

Sample type	T _{begin}	T _{live} (s)	T _{real} (s)	Geom. (cm)
Coal fly ash (1633b)	12:14PM	3600.000	3632.000	2.000
800Tat. 5 th	13:38PM	3600.000	3625.000	2.000
600Tat. 6 th	15:04PM	3600.000	3616.360	2.000
200Tat. 3 rd	09:16AM	3600.000	3612.320	2.000
4 th Tat. 1HYS	10:24AM	3600.000	3611.840	2.000
100Tat. 2 nd	11:32AM	3600.000	3611.340	2.000

Table 10: Counting schedules for 2nd sets of Six Archaeological Samples after 5 days

Sample type	T _{begin}	T _{live} (s)	T _{real} (s)	Geom. (cm)
3 rd Tat. 2YS	09:26AM	3600.00	1851.42	2.000
1 st Tat. MRB	10:01AM	3600.00	1879.42	2.000
2 nd Tat. AHM3	10:34AM	3600.00	1838.64	2.000
45 Tat. 1 st	11:07AM	3600.00	1834.66	2.000
400Tat. 4 th	11:39AM	3600.00	1855.38	2.000
IAEA lake sediment	12:12PM	3600.00	1830.84	2.000

The experimental and theoretical values compared very well with deviation of 2.86E-02 in B-2 and 3.31E-02 in A-3 respectively. These results showed that the comparator factor F_C is proportional to the epithermal neutron flux and is independent of monitor element. It tells us how correct the thermal and epithermal neutron flux obtained in this work and gives information on flux gradients and flux stability in the Cd-lined channel A-3 and B-2 inner channel.

The Rad Pro Calculator was employed and the values of the activities in Bq were entered to convert to dose-rate along side with distances and units of interest. The activities (Bq) of each of the isotopes; ^{42}K , $^{233}\text{Th}/^{233}\text{Pa}$ and $^{239}\text{U}/^{239}\text{Np}$ were entered and the dose rate in millirad per year evaluated as shown in Table 11 below.

Table 11: Results of dose rate of K, U and Th in the Ten Sediments Samples

Sample ID	Peak Energy (keV)	Nuclear Reaction	Dose rate mrad/yr
800 Tat.5 th	1524.00	$^{41}\text{K}(\text{n},\gamma)^{42}\text{K}$	0.003±1.300
	312.000	$^{232}\text{Th}(\text{n p})^{233}\text{Th}/^{233}\text{Pa}$	0.551±2.300
	277.000	$^{238}\text{U}(\text{n p})^{239}\text{U}/^{239}\text{Np}$	0.927±1.100
600 Tat.6 th	1524.000	$^{41}\text{K}(\text{n},\gamma)^{42}\text{K}$	0.002±1.300
	312.000	$^{232}\text{Th}(\text{n p})^{233}\text{Th}/^{233}\text{Pa}$	0.536±1.300
	277.000	$^{238}\text{U}(\text{n p})^{239}\text{U}/^{239}\text{Np}$	0.881±1.200
200 Tat.3 rd	1524.000	$^{41}\text{K}(\text{n},\gamma)^{42}\text{K}$	(7.130E±0.300)-04
	312.000	$^{232}\text{Th}(\text{n p})^{233}\text{Th}/^{233}\text{Pa}$	0.088±2.300
	277.000	$^{238}\text{U}(\text{n p})^{239}\text{U}/^{239}\text{Np}$	1.009±1.100
4 th Tat.1HYS	1524.000	$^{41}\text{K}(\text{n},\gamma)^{42}\text{K}$	(5.749E±0.300)-04
	312.000	$^{232}\text{Th}(\text{n p})^{233}\text{Th}/^{233}\text{Pa}$	0.139±2.300
	277.000	$^{238}\text{U}(\text{n p})^{239}\text{U}/^{239}\text{Np}$	0.541±1.100
100 Tat.2 nd	1524.000	$^{41}\text{K}(\text{n},\gamma)^{42}\text{K}$	(6.530E±0.300)-04
	312.000	$^{232}\text{Th}(\text{n p})^{233}\text{Th}/^{233}\text{Pa}$	0.073±2.300
	277.000	$^{238}\text{U}(\text{n p})^{239}\text{U}/^{239}\text{Np}$	0.794±1.100
400 Tat.4 th	1524.000	$^{41}\text{K}(\text{n},\gamma)^{42}\text{K}$	0.013±1.300
	312.000	$^{232}\text{Th}(\text{n p})^{233}\text{Th}/^{233}\text{Pa}$	0.536±1.300
	277.000	$^{238}\text{U}(\text{n p})^{239}\text{U}/^{239}\text{Np}$	0.881±1.200
45 Tat.1 st	1524.000	$^{41}\text{K}(\text{n},\gamma)^{42}\text{K}$	(5.84E±1.300)-04
	312.000	$^{232}\text{Th}(\text{n p})^{233}\text{Th}/^{233}\text{Pa}$	0.049±2.300
	277.000	$^{238}\text{U}(\text{n p})^{239}\text{U}/^{239}\text{Np}$	0.569±1.100
3 rd Tat.2YS	1524.000	$^{41}\text{K}(\text{n},\gamma)^{42}\text{K}$	0.003±1.300
	312.000	$^{232}\text{Th}(\text{n p})^{233}\text{Th}/^{233}\text{Pa}$	0.551±2.300
	277.000	$^{238}\text{U}(\text{n p})^{239}\text{U}/^{239}\text{Np}$	0.927±1.100
1 st Tat.MRB	1524.000	$^{41}\text{K}(\text{n},\gamma)^{42}\text{K}$	(5.564E±1.300)-04
	312.000	$^{232}\text{Th}(\text{n p})^{233}\text{Th}/^{233}\text{Pa}$	0.057±2.300
	277.000	$^{238}\text{U}(\text{n p})^{239}\text{U}/^{239}\text{Np}$	0.640±1.100
2 nd Tat.AHM	1524.000	$^{41}\text{K}(\text{n},\gamma)^{42}\text{K}$	(3.094E±1.300)-04
	312.000	$^{232}\text{Th}(\text{n p})^{233}\text{Th}/^{233}\text{Pa}$	0.056±2.300
	277.000	$^{238}\text{U}(\text{n p})^{239}\text{U}/^{239}\text{Np}$	0.461±1.100

100 rad/yr = Gy/yr

The results of the activity Bq obtained for Th, U and K as well as the annual dose rate for the ten archaeological samples obtained from Tatiko village of Paikoro local

Government area of Niger state Nigeria are shown in Table 12.

Table 12: Activity and Annual Dose Rate for the Ten Archaeological Samples

Sample Type	Weight, (g)	Activity of K, Bq	Activity of U/Np, Bq	Activity of Th/Pa, Bq	Dose Rate mrad/yr
800 Tat.5th	0.645	363.800	25.860	71.310	1.480±03
600Tat.6th	0.613	179.060	24.560	69.350	1.420±1.3
45 Tat.1st	0.646	63.800	15.860	6.310	(6.190E±4.300)-01
1st Tat.MRB	0.536	60.800	17.850	7.410	(6.980E±9.300)-01
2nd Tat.AHM3	0.626	33.800	12.830	7.310	(5.18E±6.300)-01
200Tat.3rd	0.606	77.420	28.140	11.440	1.380±1.300

400Tat.4th	0.506	179.060	24.560	69.350	1.420±1.400
100Tat.2nd	0.623	70.420	22.140	9.440	(8.680E±2.300)-01
4th Tat.1HYS	0.614	62.830	15.090	40.890	(3.810E±0.500)-01
3rd Tat.2YS	0.538	363.800	25.760	71.310	1.480±2.200

A graphical representation of total dose rate in mrad/hr due to $^{233}\text{Th}/^{233}\text{Pa}$, $^{239}\text{U}/^{239}\text{Np}$, and ^{42}K for the ten archeological samples is shown in Figure 4.54 for the sample ID; A (800Tat.5th), B (600Tat.6th), C (45 Tat.1st),

D (1st Tat.MRB), E (2nd Tat.AHM3), F (200Tat.3rd), G (400Tat.4th), H (100Tat.2nd), I (4th Tat.1HYS), and J (3rd Tat.2YS).

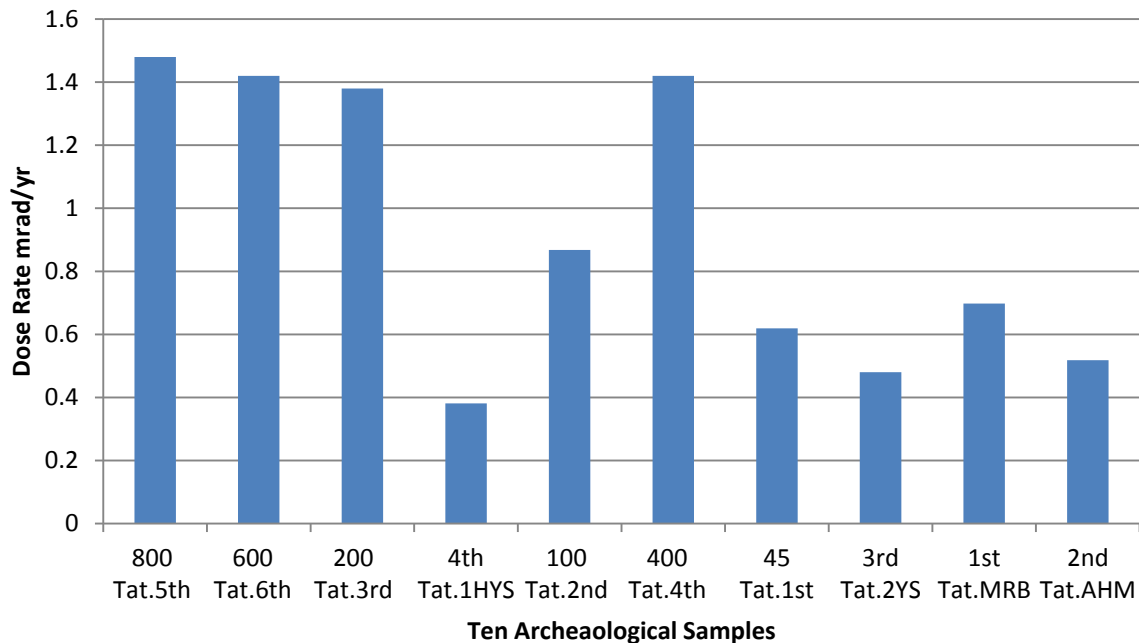


Figure 1: Total Dose Rate in the Ten Archeological Samples obtained from Tatiko village

From Figure 1, the dose rate appears to be high for sample 800Tat.5th obtained at a depth of approximately 800 cm beneath the earth surface. This trend follows suits for sample 600Tat.6th obtained at ~600 cm, 400Tat.4th obtained at about 400 cm, 200 Tat.3rd obtained ~200 cm, 100Tat. 2nd obtained ~100 cm and 45Tat.1st obtained 45cm beneath the earth surface. This shows work revealed that dose rate increases inwardly from the earth surface. Also, the dose was relatively high for sample 1stTat.MRB compared to 2ndTat.AHM. Thus, the 1stTat.MRB was obtained from the molded clay pot that was ready and was awaiting firing while 2ndTat.AHM was the clay pot that was fired. This demonstrates the knowledge of zeroing or resetting of electron growth due to availability of natural radionuclides; Th, U and K. This because those samples that were approximately 100 years (4thTat.1HYS), 2 years old (3rdTat.2YS) had relatively low doses.

5. CONCLUSION

The experimental and theoretical evaluation of the comparator factor F_c in this work showed good agreement with a deviation value of $2.86\text{E}-02$ in the inner irradiation channel B-2 (without Cd-lined) and $3.31\text{E}-02$ in the outer irradiation channel A-3 (with Cd-lined). These results showed that the neutron flux distribution of Nigeria Research Reactor-1 is very stable and the efficiency values obtained via k_0 -IAEA program (Njinga *et al.*, 2011) for the high purity germanium detector at 2 cm and 17 cm geometry, data-entry, decay time (dead time < 6 %) employed in this work are accurate. The ten samples obtained from Tatiko village Paikoro local Government Area analyzed with k_0 -IAEA program within three to five days revealed that dose rate due to U/Np, Th/Pa and K increases inwardly from the earth surface.

REFERENCES

- [1] Balogun, G.I. (2003). On safety related calculations associated with miniature neutron source reactor core conversion studies, *J. Appld. Sci & Tech.* 8, 8-13.
- [2] De Corte F., Dejaeger M., Hossain S. M., Vandenberghe D., De Wispelaere A., Van den Haute P. (2004). *A performance comparison of k_0 -based ENAA and NAA in the (K, Th, U) radiation dose rate assessment for the luminescence dating of sediments.* *Journal of Radioanalytical and Nuclear Chemistry*, Vol. 263, No. 3 (2005) 659.665
- [3] De Corte, F., Simonits, A. (1996). *KAYZERO/SOLOCI for Reactor Neutron Activation Analysis (NAA) using the k_0 Standardization Method Version 4 User's Manual.* DSM Research, Geleen (NL).
- [4] Erdtmann, G., Soyka, W. (1979). *The γ -Rays of the Radionuclides; Tables for Applied γ -Ray Spectrometry (vol.7).* Verlag Chemie: Weinheim, New York, 1-236.
- [5] Glascock, M.D (1988). *Tables for Neutron Activation Analysis.* The University of Missouri, Columbia.
- [6] Jonah, S.A., Balogun, G.I., Umar, M. I., Mayaki, M.C., (2005). *Neutron spectrum parameters in irradiation channels of the Nigeria Research Reactor-1 (NIRR-1) for k_0 -NAA standardization.* *Journal of Radioanalytical and nuclear chemistry*, Vol.266 (1) P 83-88.
- [7] Njinga, R. L. Ibrahim, Y. V., Adeleye, M.O., and Jonah, S.A (2012): Determination of flux parameters after installation of Cd-lined for implementation of ENAA and FNAA with NIRR-1, *International Journal of Applied Science and Technology* Vol 2, pg 186-196
- [8] Njinga, R.L., Jonah, S.A., Ewa, I.O.B., Oladipo, M.O.A., and Agbo, G.A. (2011). *k_0 -IAEA determination of full energy peak efficiency for a high purity germanium detector.* *Indian J.Sci.Res.* (3):25-32